SARM1 participates in axonal degeneration and mitochondrial dysfunction in prion disease
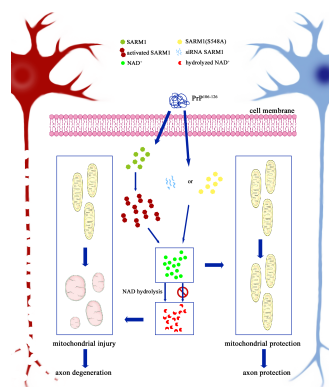
Meng-Yu Lai, Jie Li, Xi-Xi Zhang, Wei Wu, Zhi-Ping Li, Zhi-Xin Sun, Meng-Yang Zhao, Dong-Ming Yang, Dong-Dong Wang, Wen Li, De-Ming Zhao, Xiang-Mei Zhou[*], Li-Feng Yang[*]

From the Contents

Graphical Abstract *NAD⁺-hydrolase activity of SARM1 regulates PrP[106–126]-induced axonal degeneration and mitochondrial dysfunction*

Abstract

Prion disease represents a group of fatal neurogenerative diseases in humans and animals that are associated with energy loss, axonal degeneration, and mitochondrial dysfunction. Axonal degeneration is an early hallmark of neurodegeneration and is triggered by SARM1. We found that depletion or dysfunctional mutation of SARM1 protected against NAD⁺ loss, axonal degeneration, and mitochondrial functional disorder induced by the neurotoxic peptide PrP[106–126]. NAD⁺ supplementation rescued prion-triggered axonal degeneration and mitochondrial dysfunction and SARM1 overexpression suppressed this protective effect. NAD⁺ supplementation in PrP[106–126]-incubated N2a cells, SARM1 depletion, and SARM1 dysfunctional mutation each blocked neuronal apoptosis and increased cell survival. Our results indicate that the axonal degeneration and mitochondrial dysfunction triggered by PrP[106–126] are partially dependent on SARM1 NADase activity. This pathway has potential as a therapeutic target in the early stages of prion disease.

Key Words: axonal degeneration; mitochondrial dysfunction; NAD⁺ metabolism; NADase; neurodegenerative disease; prion disease; SARM1; sterile alpha and TIR motif-containing 1

Introduction

Prion disease represents a group of transmissible and fatal neurogenerative diseases in both animals and humans that includes scrapie, bovine spongiform encephalopathy, and Creutzfeldt-Jakob disease (Collinge, 2001). Accumulation of the misfolded form of the cellular prion protein in the central nervous system induces neuronal loss, spongiform vacuolation, and inflammation and is the main cause of neurodegeneration (Prusiner, 1991; Hur et al., 2002; Soto and Satani, 2011; Batlle and Ventura, 2020). The misfolded cellular prion protein is termed PrP^Sc. Prion protein peptide 106–126 (PrP[106–126]), a neurotoxic prion protein fragment, has been used by researchers to mimic amyloid-like fibril accumulation and trigger axonal degeneration and neuronal apoptosis *in vitro* (Prusiner, 1991; Soto and Satani, 2011; Forloni et al., 2019; Groveman et al., 2020; Ishikawa et al., 2021).

In studies of various neurodegenerative diseases, the loss of synapses and axons that precedes neuronal loss is adequate to cause clinical symptoms (Li et al., 2001; Gunawardena and Goldstein, 2005; Luo and O'Leary, 2005; Stokin and Goldstein, 2006; Gerdts et al., 2015). Therefore, axonal degeneration is considered a hallmark of neurodegenerative disorders (Soto and Satani, 2011). Mitochondria are the most important cellular hub for adenosine triphosphate (ATP) production, the key source of cellular energy. Neurons are especially sensitive to mitochondrial dysfunction due to their extreme dependence on mitochondria for energy (Galluzzi et al., 2012; Morán et al., 2012). During ATP biosynthesis, nicotinamide adenine dinucleotide (NAD⁺) functions as an irreplaceable coenzyme. In previous studies, researchers found that the fifth member of the myeloid differentiation primary response 88 family, sterile alpha and Toll-interleukin receptor 1 receptor (TIR) motif-containing 1 (SARM1), was required for axonal degeneration induced by axotomy. In addition, SARM1 knockout rescued symptoms in both *in vivo* and *in vitro* models (Osterloh et al., 2012; Henninger et al., 2016). Because injury-induced axonal degeneration has been associated with reduced NAD⁺ concentration, SARM1 may regulate this degeneration via a gain of NAD⁺ cleavage activity following release of SARM1 autoinhibition and dimerization of its TIF domains (Wang et al., 2005; Gerdts et al., 2015).

Neuronal death and axonal degeneration in prion disease are linked with NAD⁺ depletion (Wang et al., 2015) and can be relieved by NAD⁺ replenishment. In a previous study, we investigated prion disease-induced mitochondrial dysfunction in both cell line and animal models (Wu et al., 2019). Because mitochondria process NAD⁺ to synthesize ATP and SARM1 can link to the outer mitochondrial membrane via its mitochondrial targeting sequence domain (Panneerselvam et al., 2012), we hypothesized that axonal degeneration associated with prion disease is partially regulated by SARM1 protein activation and its subsequent destruction of NAD⁺. To verify this hypothesis, we examined the effect of SARM1 knockdown/null mutation on the NAD⁺ depletion, mitochondrial dysfunction, and axonal degeneration induced by treatment with PrP[106–126]. In addition, we determined the effect of NAD⁺ replenishment on mitochondrial dysfunction and mitochondrial and axonal morphology in cells incubated with PrP[106–126].

Materials and Methods

Ethics statement
All animals in this study were treated in accordance with the Guidelines

National Animal Transmissible Spongiform Encephalopathy Laboratory, College of Veterinary Medicine, China Agricultural University, Beijing, China
*Correspondence to: Li-Feng Yang, PhD, yanglf@cau.edu.cn; Xiang-Mei Zhou, PhD, zhouxm@cau.edu.cn.
https://orcid.org/0000-0001-5175-7589 (Li-Feng Yang); https://orcid.org/0000-0003-1566-5745 (Xiang-Mei Zhou)

How to cite this article: Lai MY, Li J, Zhang XX, Wu W, Li ZP, Sun ZX, Zhao MY, Yang DM, Wang DD, Li W, Zhao DM, Zhou XM, Yang LF (2022) SARM1 participates in axonal degeneration and mitochondrial dysfunction in prion disease. Neural Regen Res 17(10):2293-2299.

of the China Agricultural University on the Review of Welfare and Ethics of Laboratory Animals. The study protocol was approved by the China Agricultural University Administration Office of Laboratory Animals (approval No. AW02011202-2-1) on September 1, 2020.

Cell culture and treatment
Primary neurons were prepared from the cerebral cortex of 1-day-old neonatal Sprague-Dawley rats (SPF (Beijing) Biotechnology Co., Ltd. Beijing, China; license No. SCXK (Jing) 2016-0002) following a previously described procedure (Song et al., 2016). Neonatal rats were sacrificed by decapitation. Neurons were dissociated from cerebral cortex tissue after digestion by using Dulbecco's modified Eagle's medium (Hyclone, Logan, UT, USA) with papain (2 mg/mL, Invitrogen, Carlsbad, CA, USA) and DNAse (50 mg/mL; Sigma-Aldrich, St. Louis, MO, USA) for 30 minutes at 37°C. The cells were plated and pre-incubated with L-polylysine (Solarbio, Beijing, China) at the appropriate concentration for different uses. Primary cortical neurons were cultured in a specific culture medium comprising Neurobasal-A Medium (Invitrogen) with 2% serum-free B27 supplement (Invitrogen) and 0.5% penicillin-streptomycin (Gibco, Grand Island, NY, USA). The medium was replaced every 2 days in half of the volume to satisfy the nutritional requirements for cell growth. The experimental processes were performed after 1 week of culture. Culture medium used for mouse neuroblastoma (N2a) cells (National Infrastructure of Cell Line Resource, Beijing, China; ATCC Cat# CCL-131, RRID: CVCL_0470) was based on Dulbecco's modified Eagle's medium containing 10% (v/v) fetal bovine serum (Gibco) and 1% penicillin-streptomycin (Gibco). Primary neurons and N2a cells were cultured at 37°C in a humid incubator with 5% CO_2.

PrP peptide PrP[106–126] (sequence: KTNMKKHMAGAAAAGAVVGGLG; 98% purity; Sangon Bio-Tech, Beijing, China) was dissolved in phosphate-buffered saline (PBS; Solarbio) to form a 1 mM storage solution. After being shaken at 4°C for 24 hours, the solution could be stored at 4°C for a short period. Primary neurons or N2a cells were incubated with the peptide for 3, 6, 12, or 24 hours as described in the results. The final peptide concentration in experiment processing was 200 μM.

β-Nicotinamide adenine dinucleotide (β-NAD; Sigma-Aldrich) was dissolved in PBS to a storage concentration of 15 μm/mL and stored away from light at −20°C. Primary neurons or N2a cells were incubated with β-NAD for 12 hours with PrP peptide.

Small interfering RNA, plasmids, and transfection
The SARM1 small interfering RNA (siRNA; 5′-GGT AGA TGG TGA TTT GCT T-3′), pCMV-SARM1 plasmid, and pCMV-SARM1(S548A) plasmid were obtained from SYKMGENE (Beijing, China). Primary neurons were transfected with antibiotic-free Dulbecco's modified Eagle's medium containing 500 ng siRNA, 0.75 μL Lipofectamine 3000, and 50 μL Opti-MEM (both from Invitrogen) per 500 μL cell culture medium for 48 hours. N2a cells were transfected with siRNA using the same reagent system for 48 hours or with siRNA for 12 hours as a protein knockdown background and then transfected with the SAMR1 plasmid or SARM1(S548A) plasmid using the same reagent system but with adding 1 μL P3000 reagent (Invitrogen) per 500 μL culture medium for 48 hours.

Western blot assay
Both primary neurons and N2a cells were harvested after the experimental processes using lysis buffer (Beyotime, Shanghai, China) containing 1% protease inhibitor solution (Beyotime). The lysed cells were collected and cultured with lysis buffer in Eppendorf tubes and centrifuged at 12,000 × g for 10 minutes at 4°C. The supernatants were then transferred to new tubes. The samples were used for western blotting after boiling with loading buffer (Solarbio).

Proteins were separated on sodium dodecyl sulfate-polyacrylamide gels according to molecular weight and then transferred onto a nitrocellulose membrane (Sigma-Aldrich). After culturing with 5% skim milk dissolved in Tris-buffered saline containing 0.1% Tween 20, the samples were placed in blocking buffer at 37°C for 1 hour. Individual primary antibodies were incubated at appropriate concentrations at 4°C overnight, including rabbit anti-SARM1 (Abcam, Cambridge, UK, Cat# ab226930, RRID: AB_2893433, 1:1000), mouse anti-neuronal class III tubulin (TU20; CST, Danvers, MA, USA, Cat# 4466, RRID: AB_1904176, 1:1000), mouse anti-neuronal class III tubulin (Tuj1; Beyotime, Cat# AT809, RRID: AB_2893434, 1:500), and mouse anti-glyceraldehyde-3-phosphate dehydrogenase (Proteintech, Rosemont, IL, USA, Cat# 60004-1-Ig, RRID: AB_2107436, 1:10,000). After each membrane was washed with Tris-buffered saline containing 0.1% Tween 20, it was incubated with relevant secondary antibodies, including goat anti-mouse IgG conjugated to horseradish peroxidase (ZSGB-Bio, Beijing, China, Cat# ZB2305, RRID: AB_2747415, 1:10,000) and goat anti-rabbit IgG conjugated to horseradish peroxidase ZSGB-Bio, Cat# ZB2301, RRID: AB_2747412, 1:10,000). The membranes were imaged using a gel imaging system (Tanon, Shanghai, China) and results were normalized to glyceraldehyde-3-phosphate dehydrogenase. Images were analyzed using ImageJ software version 1.52a (National Institutes of Health, Bethesda, MD, USA) (Schneider et al., 2012).

Immunofluorescence staining
Primary neurons were seeded on 24-well cell culture plates with cover slips pre-incubated with L-polylysine (Solarbio) after the dissociation steps described above. After experimental treatment, cells were softly washed with PBS and bathed with Immunolo Staining Fix Solution (Beyotime), followed by Immunol Permeabilization Buffer (Beyotime) at room temperature for 10 minutes, and Immunol Staining Blocking Buffer (Beyotime) at room temperature for 1 hour. Primary antibody incubations were processed at 4°C overnight followed by relevant secondary antibody incubations at 37°C for 1 hour. Primary neuronal axons were labelled using a mouse anti-TU20 antibody (a marker of primary neuronal axons; CST, Cat# 4466, RRID: AB_1904176, 1:1000) and an Alexa Fluor 488 labeled goat anti-mouse IgG (H+L) (Beyotime, Cat# A0428, RRID: AB_2893435, 1:400). Mitochondria in primary neurons were labelled using rabbit anti-translocase of outer mitochondrial membrane 40 (TOMM40) antibody (Proteintech, Cat# 18409-1-AP, RRID: AB_2303725, 1:1000) and Alexa Fluor 555-labeled donkey anti-rabbit IgG (H+L) antibody (Beyotime, Cat# A0453, RRID: AB_2890132, 1:400). All slides were photographed using a Nikon (Tokyo, Japan) confocal imaging system. Images were analyzed using ImageJ software version 1.52a.

Determination of mitochondrial function
The JC-1 mitochondrial membrane potential (MMP) assay kit (Beyotime) was used to detect the MMP. The N2a cells were harvested after experimental processes, collected into a tube after washing softly by PBS, and then incubated with the JC-1 probe for 30 minutes at 37°C. After washing with the wash buffer from the kit, the samples were analyzed using flow cytometry. The ATP determination kit (Beyotime) was used to measure cellular ATP level, which was performed at low temperature. Cells in the culture plate were lysed with the lysis buffer from the kit and incubated in black 96-well plates with 100 μL detection reagent; 50 μL samples were added to each well. Luminescence of each well was measured using a luminometer (TECAN, Männedorf, Austria).

Measurement of NAD level
The NAD/NADH-Glo assay kit (Promega, Madison, WI, USA) was used to determine cellular NAD. After experimental processes, N2a cells were re-seeded at a concentration of 30,000 cells/well in flat white 96-well plates and incubated with detection reagent preformed as guidance of manufacturer instructions for 30 minutes. Luminescence was recorded using a plate stacker (TECAN).

Cell viability assay
The Cell Counting Kit-8 assay kit (Beyotime) was used to determine N2a cell viability after experimental processes. The kit detection reagent was diluted with cell culture medium according to manufacturer instructions and incubated with the cells for 1 hour under cell culture conditions in a humid incubator. Using a cell-free sample as blank control, the absorbance at 450 nm was determined using a microplate reader (Thermo, Waltham, MA, USA). Cell viability was expressed as a percentage of the untreated control sample (100%).

TdT-mediated dUTP nick-end labeling assay
N2a cells were seeded on cover slips in a 24-well plate. After the experimental treatments, the One Step TdT-mediated dUTP nick-end labeling (TUNEL) Apoptosis Assay Kit (Beyotime) was used. This procedure was performed away from light. The samples were prepared as described for immunofluorescence microscopy until antibody incubation. Then, the samples were incubated with TUNEL stain reagent for 1 hour at 37°C. 4′,6-Diamidino-2-phenylindole stain reagent (Beyotime) was used to visualize the nucleus for 10 minutes at 37°C. All slides were photographed using a Nikon confocal imaging system. Images were analyzed using ImageJ software version 1.52a.

Statistical analysis
Data are expressed as means ± standard error of the mean (SEM) and were analyzed using one-way analysis of variance followed by Bonferroni's *post hoc* test. Analyses were performed using Prism 5.0 software (GraphPad Software, La Jolla, CA, USA). $P < 0.05$ was considered significant.

Results

Axonal degeneration induced by PrP[106–126] incubation
In prion disease, the most characteristic pathological change is neuronal degeneration, which causes dramatic clinical symptoms (Prusiner, 1991; Hur et al., 2002; Soto and Satani, 2011). Neuronal cell damage in prion disease models has been investigated in our previous studies (Wang et al., 2015; Song et al., 2016), which focused on morphological changes in the ultrastructure of primary cultured cortical neurons and axonal loss by spinal cord neurons after PrP[106–126] incubation. We found that the axons of primary cultured cortical neurons were severely shortened after 12 hours of incubation with 200 μM PrP[106–126] peptide (**Figure 1A** and **B**). In N2a cells, the expression level of beta-tubulin III, a neuron-specific type of tubulin (Gerdts et al., 2013), was reduced remarkably by the same treatment (**Figure 1C** and **D**). These results demonstrate that 12 hours of incubation with PrP106-126 caused axonal degeneration in primary cultured cortical neurons and decreased beta-tubulin III expression in N2a cells.

SARM1 is required for PrP[106–126]-induced axonal degeneration
In recent studies of neurodegenerative diseases, the role of SARM1 in axonal degeneration has gradually become clearer (Osterloh et al., 2012; Gerdts et al., 2013; Henninger et al., 2016; Essuman et al., 2017). To determine whether SARM1 is involved in axonal degeneration induced by PrP[106–126] incubation, we first examined the level of SARM1 expression in N2a cells. According to our western blot results, SARM1 expression was increased significantly in N2a cells treated with PrP[106–126] for 12 or 24 hours (**Figure 2A** and **B**). Since SARM1-expressing neurons showed decreased expression of beta-tubulin III after treatment with PrP[106–126], we explored the role of SARM1 in this effect with SARM1 knockdown using siRNA (**Figure 2C**). Western blotting showed
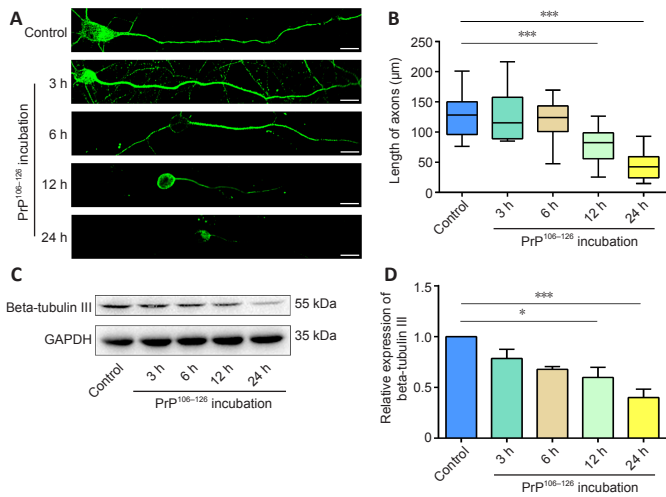
Figure 1 | PrP106–126 triggers axonal degeneration in primary cultured neurons and N2a cells.
(A) Rat primary cultured neurons were incubated with 200 μM PrP106–126 for 3, 6, 12, or 24 hours. Neuronal structure was photographed after immunofluorescence staining with anti-TU20 (green, stained by Alexa Fluor 488). Scale bars: 10 μM. Axon length declined significantly after incubation with 200 μM PrP106–126 for 12 and 24 hours. (B) Analysis of axon length after PrP106–126 incubation. (C) Western blot bands of beta-tubulin III in PrP106–126-treated N2a cells. (D) Quantitative results of tubulin III expression, which was normalized to the control group. Expression of beta-tubulin III declined significantly after incubation with 200 μM PrP106–126 for 12 and 24 hours. Data are expressed as means ± SEM. All assays were repeated three times. *$P < 0.05$, ***$P < 0.001$, *vs.* control group (one-way analysis of variance followed by Bonferroni's *post hoc* test). GADPH: Glyceraldehyde-3-phosphate dehydrogenase; PrP106–126: PrP peptide 106–126; TU20: neuronal class III tubulin.

that SARM1 knockdown N2a cells maintained their level of beta-tubulin III following treatment with PrP106–126 (**Figure 2D** and **E**). Next, we overexpressed full-length SARM1 using plasmid transfection (500 ng for 48 hours) in SARM1 knockdown N2a cells (**Figure 2F**) and showed that treatment with PrP106–126 reduced the beta-tubulin III expression level of the transfected cells (**Figure 2G** and **H**). In addition, SARM1 knockdown (**Figure 2I**) protected the axonal structure of primary cultured cortical neurons during PrP106–126 incubation (**Figure 2J** and **K**). Our findings indicate that SARM1 is involved in axonal degeneration caused by PrP106–126 and that knockdown of SARM1 protects neurons from this pathological change.

PrP106–126-induced mitochondrial morphological damage and dysfunction are partly mediated by SARM1
Considering that neurons consume a large amount of energy, mitochondria are critical organelles involved in many neurodegenerative diseases (Pacelli et al., 2015; Swerdlow, 2018; Wang et al., 2021). In our previous studies, mitochondrial fragmentation and dysfunction were observed in prion disease models (Li et al., 2018; Wu et al., 2019; Zhang et al., 2020). In other studies, SARM1 function was also associated with mitochondrial respiration and mitochondrial dysfunction-induced cell death (Summers et al., 2014; Murata et al., 2018). Therefore, we hypothesized that SARM1 plays a role in PrP106–126-induced axonal degeneration via regulation of mitochondrial function. After incubation with 200 μM PrP106–126 for 12 hours, mitochondria in primary cultured cortical neurons were imaged using fluorescence microscopy. TOMM40 staining showed that PrP106–126-treated neurons had a remarkably fragmented mitochondrial network, whereas untreated control neurons had filamentous, continuous mitochondria, which suggested mitochondrial changes. The mitochondria of primary neurons that were treated with SARM1 siRNA and then incubated with PrP106–126 maintained their tubular morphology (**Figure 3A**). Mitochondrial length decreased significantly in PrP106–126-treated neurons; however, in PrP106–126-treated SARM1-knockdown neurons, the length significantly recovered (**Figure 3B**). To ascertain mitochondrial function, we measured the ATP level of PrP106–126-treated N2a cells. After PrP106–126 incubation, the ATP level of N2a cells was reduced to approximately 50% of that of control. PrP106–126-induced ATP loss was prevented by SARM1 knockdown and accelerated by overexpression of SARM1 (**Figure 3C**).

MMP loss is also a signal of mitochondrial dysfunction; therefore, we assessed the MMP using the JC-1 assay. The monomer form of JC-1 in damaged mitochondria appears green, while the aggregate form in healthy mitochondria appears red. The red/green ratio reflects the MMP and would decrease with MMP loss. In concert with the ATP measurements mentioned above, PrP106–126 incubation lowered the MMP compared with the untreated control. The change in MMP induced by PrP106–126 incubation was prevented by SARM1 knockdown and aggravated by SARM1 overexpression (**Figure 3D**). These results indicate that SARM1 takes part in the mitochondrial morphology changes and dysfunction induced by PrP106–126 incubation.

PrP106–126-induced mitochondrial dysfunction and axon degeneration via the NAD+-hydrolase activity of SARM1
In a previous study, Wang et al. (2015) proposed NAD+ replenishment for

neuroprotection in patients with prion disease. Because SARM1 performs cleavage of NAD+, which has been associated with axonal degeneration (Gerdts et al., 2015; Essuman et al., 2017), we conjectured that SARM1 mediates axonal degeneration and mitochondrial dysfunction via its NAD+ hydrolase activity. We found that PrP106–126 incubation destroys approximately 50% of cellular NAD+. In cells incubated with PrP106–126 and treated with SARM1 siRNA, the NAD+ level was similar to that in control cells; however, cells overexpressing SARM1 showed enhanced loss of NAD+ (**Figure 4A**). Next, we investigated the effects of NAD+ supplementation on axonal and mitochondrial morphology in an *in vitro* prion model by observing β-NAD-treated primary neurons using fluorescence microscopy. In primary cultured cortical neurons incubated with PrP106–126, the mitochondria of β-NAD-treated cells maintained their filamentous and tubular shape and longer average length compared with the fragmented mitochondria of the PrP106–126-treated group (**Figure 4B** and **C**). ATP level and MMP were measured to assess mitochondrial function. The ATP level in PrP106–126-incubated N2a cells was increased dramatically after treatment with β-NAD. Therefore, NAD treatment protected cells from PrP106–126-induced ATP loss, even in cells overexpressing SARM1. However, SARM1 overexpression impaired recovery of the ATP level (**Figure 4D**).

In concert with the findings described above, after PrP106–126 incubation, the MMP of NAD-treated cells was maintained compared with that of cells treated with PrP106–126 only. Moreover, overexpression of SARM1 weakened the protective effect of NAD supplementation on MMP during PrP106–126 incubation (**Figure 4E**). In cells incubated with PrP106–126, axons in the β-NAD-treated group were significantly longer (**Figure 4B** and **F**). NAD+ treatment also resulted in higher expression of beta-tubulin III in N2a cells; however, and not surprisingly, overexpression of SARM1 limited the recovery of beta-tubulin III expression (**Figure 4G** and **H**).

Our results suggest that the NAD+ hydrolase activity of SARM1 plays a role in PrP106–126-induced mitochondrial dysfunction and axonal degeneration, and that NAD supplementation can prevent these deleterious effects of PrP106–126 on mitochondria and axons.

The reduced NADase activity of the SARM1(S548A) mutant limits mitochondrial dysfunction and axonal degeneration triggered by PrP106–126
To confirm that the NAD+ hydrolase activity of SARM1 is a critical factor in mitochondrial dysfunction and axonal degeneration, we obtained a plasmid containing the S548A mutant SARM1 sequence, as S548A SARM1 has reduced NAD+ cleavage activity (Murata et al., 2018). After transfecting the SARM1(S548A) plasmid into SARM1-silenced N2a cells (**Figure 5A**), we measured the intracellular NAD+ level in cells treated with PrP106–126 and cells that were not treated. NAD+ depletion induced by PrP106–126 incubation in the SARM1(S548A)-expressed N2a cells was limited and similar to that in the SARM1-silenced group but dramatically higher than that in the SARM1-overexpressed group (**Figure 5B**). Next, we measured the mitochondrial function of SARM1(S548A) N2a cells (**Figure 5C** and **D**). In contrast to cells overexpressing SARM1, SARM1(S548A) N2a cells did not show a loss of ATP or reduced MMP following PrP106–126 incubation. The intracellular ATP concentration and MMP of SARM1(S548A) N2a cells were maintained at levels similar to those in the SARM1-silenced group. Analysis of beta-tubulin III expression via western blotting yielded similar results (**Figure 5E** and **F**). Incubation with PrP106–126 did not decrease the expression of beta-tubulin III in SARM1(S548A) N2a cells. These results suggest that the NAD-hydrolase activity of SARM1 is required for SARM1-related mitochondrial dysfunction and axonal degeneration induced by PrP106–126 incubation.

SARM1 is involved in PrP106–126-induced neuronal death
Because neuronal apoptosis is a characteristic of prion disease (Forloni et al., 2019; Wu et al., 2019) and cell survival is a key clinicopathologic factor, we investigated the effect of SARM1 NAD+ hydrolase activity in cells incubated with PrP106–126. Apoptosis was assessed using the TUNEL assay in control, SARM1-silenced, SARM1-overexpressed, and SARM1(S548A)-expressed N2a cells (**Figure 6A** and **B**). The apoptotic cell percentage was increased in N2a cells following PrP106–126 incubation. This increase was prevented in SARM1-silenced cells and enhanced in SARM1-overexpressed cells. In the SARM1(S548A)-expressed group, PrP106–126 incubation failed to trigger apoptosis. Next, we assayed cell viability using the CCK8 assay (**Figure 6C**). SARM1 silencing protected PrP106–126-incubated cells from dying, while SARM1 overexpression increased the percentage of apoptotic cells. In addition, cell viability was maintained in SARM1(S548A)-expressed cells treated with PrP106–126, confirming the results of the apoptosis assays. These results indicate that the NAD+ hydrolase activity of SARM1 is critical in PrP106–126-induced cell death and that SARM1 silencing or loss of function protects against this PrP106–126 effect.

**Pharmacological supplementation with NAD+ promotes N2a survival in prion disease**
As shown in **Figure 4**, NAD+ supplementation protected mitochondrial morphology and function from the deleterious effects of PrP106–126; therefore, we assessed the effect of NAD+ supplementation on cell survival. The results of apoptosis and viability assays showed that NAD+ supplementation inhibited apoptosis induced by PrP106–126 and increased cell survival. In the SARM1-overexpressed group, NAD+ supplementation inhibited apoptosis and protected cells from cell death induced by PrP106–126; but the protective effect was limited by SARM1 overexpression (**Figure 7A–C**). These results confirm that NAD+ supplementation rescued PrP106–126-induced apoptosis and that this effect was suppressed by SARM1 overexpression.
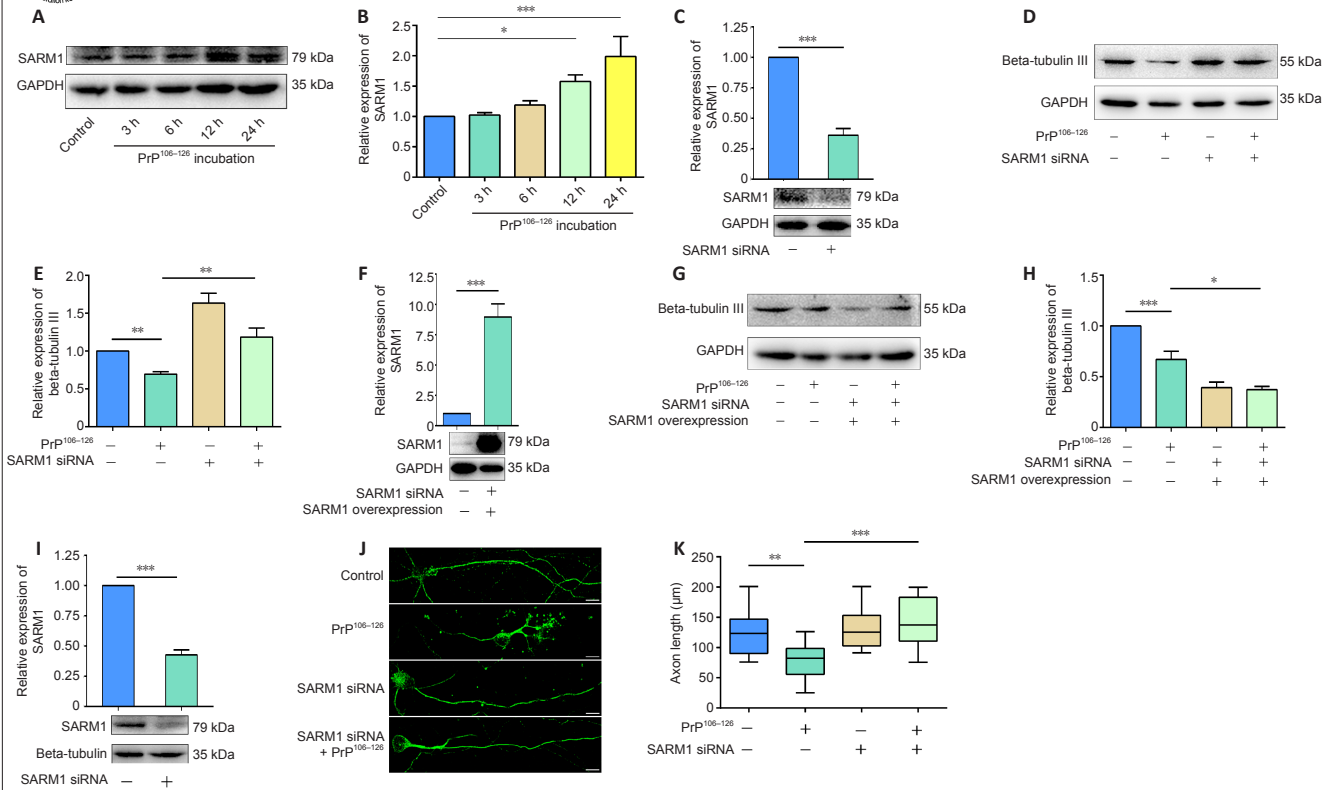
**Figure 2 | SARM1 contributes to axon degeneration in PrP^106–126^-treated cells.**
(A) Western blots of SARM1 in PrP[106–126]-treated N2a cells. (B) Quantitative results for SARM1 expression. (C) Representative western blot results for SARM1 protein in N2a cells after transfection with SARM1 siRNA for 48 hours. (D) Western blots of beta-tubulin III in SARM1 knockdown N2a cells treated with PrP[106–126] compared with control. (E) Quantitative results for the data shown in D. (F) Representative western blot results for SARM1 protein in N2a cells transfected with SARM1 plasmid for 48 hours after 12 hours SARM1 siRNA transfection. (G) Western blots of beta-tubulin III in SARM1 overexpressed N2a cells treated with PrP[106–126] compared with control. (H) Quantitative results for the data shown in G. (I) Representative western blot results for SARM1 protein in primary neurons after transfection with SARM1 siRNA for 48 hours. (J) Primary neurons were transfected with SARM1 siRNA for 48 hours before incubation with PrP[106–126]. Neuronal structure is shown in fluorescent green (stained by Alexa Fluor 488). After incubation with PrP[106–126], axonal length was shortened significantly. SARM1 knockdown protected axons from PrP[106–126]-induced degeneration. Scale bars: 10 μm. (K) Analysis of axon length. Data are expressed as the mean ± SEM. All assays were repeated three times. *$P < 0.05$, **$P < 0.01$, ***$P < 0.001$ (one-way analysis of variance followed by Bonferroni's *post hoc* test). GADPH: Glyceraldehyde-3-phosphate dehydrogenase; PrP[106–126]: PrP peptide 106–126; SARM1: sterile alpha and Toll-like receptor motif-containing 1; siRNA: small interfering RNA.
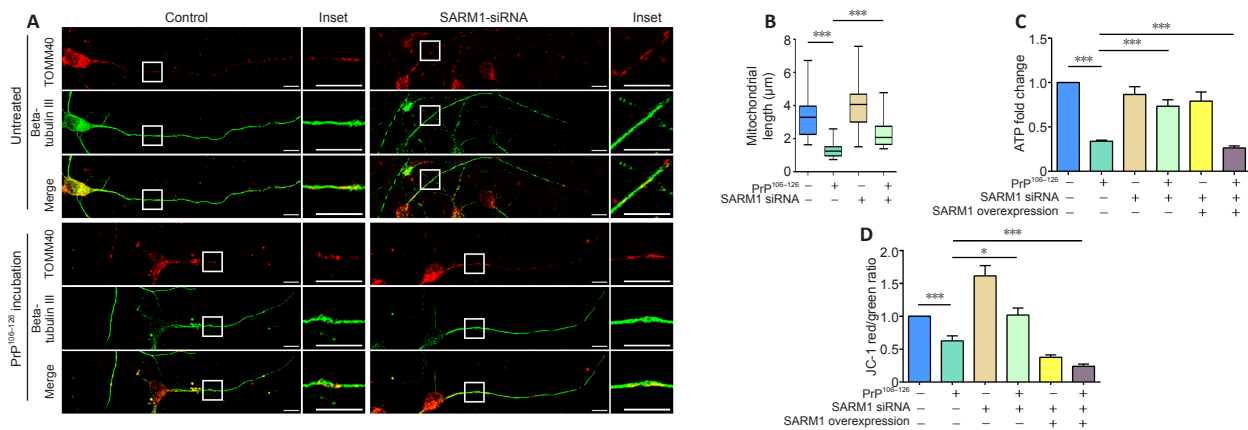

Figure 3 | SARM1 is involved in changes in mitochondrial morphology and function caused by PrP^106–126^ treatment.
(A) Primary neurons were transfected with SARM1 siRNA for 48 hours before PrP[106–126] incubation. After incubation with PrP[106–126], the mitochondrial network was fragmented; however, in the SARM1 knockdown group, mitochondria kept their tubular morphology after PrP[106–126] incubation. Neuronal structure is shown in fluorescent green (Alexa Fluor 488), while mitochondria appear red (Alexa Fluor 555). Scale bars: 10 μM. (B) Analysis of mitochondrial length. (C) Relative intracellular ATP level. Control, SARM1-silenced, and SARM1-overexpressed N2a cells were incubated with PrP[106–126]. (D) Mitochondrial membrane potential. Control, SARM1-silenced, and SARM1-overexpressed N2a cells were incubated with PrP[106–126]. Data are expressed as means ± SEM. All assays were repeated three times. *$P < 0.05$, ***$P < 0.001$ (one-way analysis of variance followed by Bonferroni's *post hoc* test). ATP: Adenosine triphosphate; PrP[106–126]: PrP peptide 106–126; SARM1: sterile alpha and Toll-like receptor motif-containing 1; siRNA: small interfering RNA; TOMM40: translocase of outer mitochondrial membrane 40.
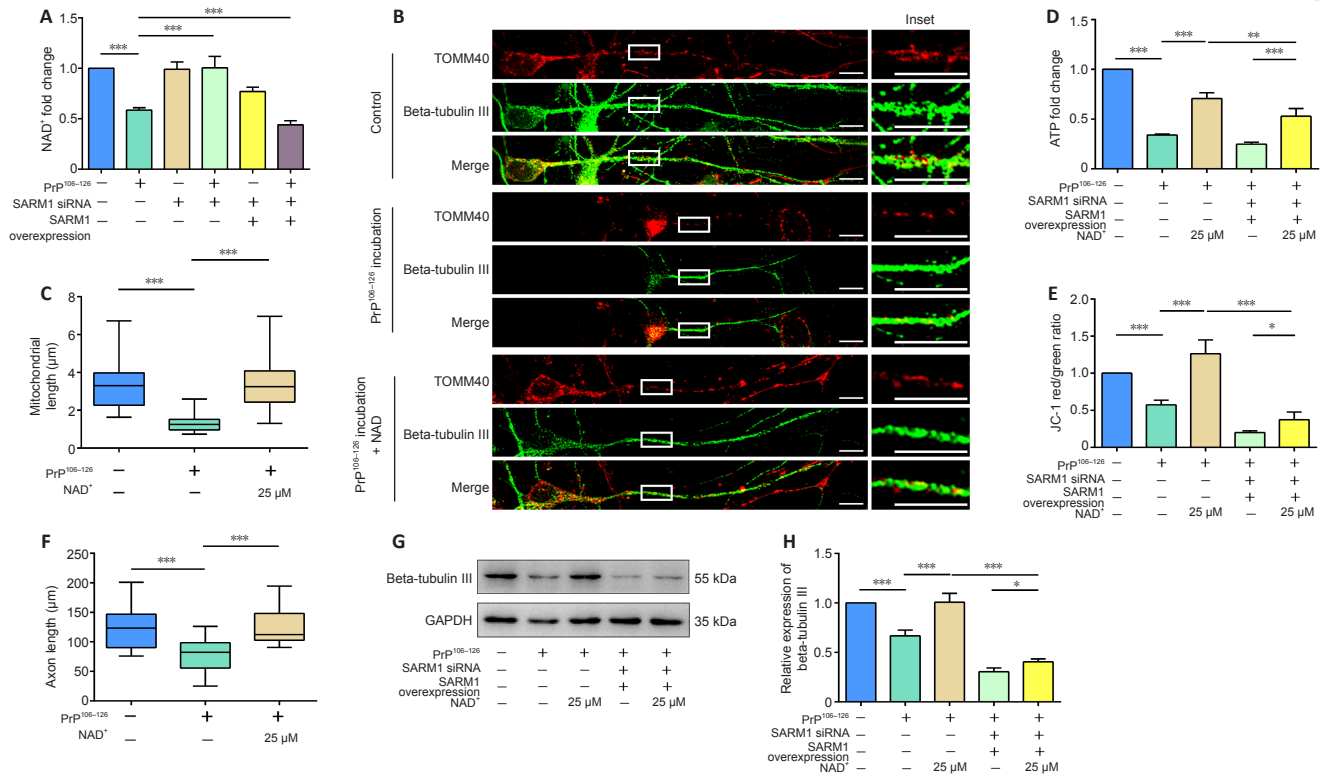
Figure 4 │ NAD-hydrolase activity of SARM1 plays a role in PrP[106–126]-induced axonal degeneration and mitochondrial disorders.

(A) Relative intracellular NAD level. Control, SARM1-silenced, and SARM1-overexpressed N2a cells were incubated with or without PrP[106–126]. (B) Primary neurons were incubated with 25 μM NAD and 200 μM PrP[106–126] for 12 hours. After PrP[106–126] incubation, the intracellular NAD level dropped significantly; however, in SARM1-silenced cells, the NAD level was protected. SARM1-overexpression enhanced the decrease in intracellular NAD. Neuronal structure is shown in fluorescent green (Alexa Fluor 488), while mitochondria appear red (Alexa Fluor 555). Scale bars: 10 μm. (C) Analysis of mitochondrial length. (D) Relative intracellular ATP levels in control and SARM1-overexpressed N2a cells incubated with PrP[106–126] with and without NAD treatment. (E) Mitochondrial membrane potential in control and SARM1-overexpressed N2a cells incubated with PrP[106–126] with and without NAD treatment. (F) Analysis of axon length. (G) Western blots of beta-tubulin III levels in control and SARM1-overexpressed N2a cells incubated with PrP[106–126] with and without NAD treatment. (H) Quantitative results of the data shown in G. Data are expressed as means ± SEM. All assays were repeated three times. *P < 0.05, **P < 0.01, ***P < 0.001 (one-way analysis of variance followed by Bonferroni's *post hoc* test). GADPH: Glyceraldehyde-3-phosphate dehydrogenase; PrP[106–126]: PrP peptide 106–126; NAD: nicotinamide adenine dinucleotide; SARM1: sterile alpha and Toll-like receptor motif-containing 1; siRNA: small interfering RNA; TOMM40: translocase of outer mitochondrial membrane 40.
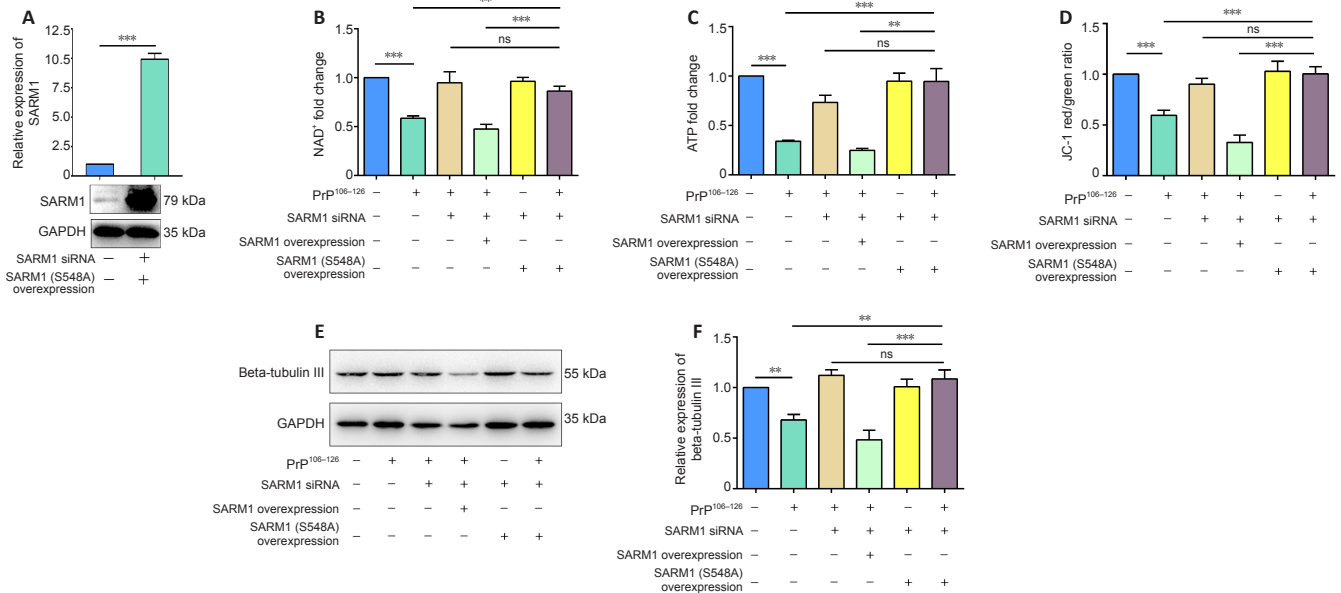
Figure 5 │ Expression of SARM1(S548A) improves mitochondrial dysfunction and reduces axonal degeneration induced by PrP[106–126].

(A) Western blot results for SARM1 protein in N2a cells transfected with the SARM1(S548A) plasmid for 48 hours after 12 hours SARM1 siRNA transfection. (B) Relative intracellular NAD level. Control, SARM1-silenced, SARM1-overexpressed, and SARM1(S548A)-expressed N2a cells were incubated with or without PrP[106–126]. (C) Relative intracellular ATP levels in control, SARM1-silenced, SARM1-overexpressed, and SARM1(S548A)-expressed N2a cells incubated with or without PrP[106–126]. (D) Mitochondrial membrane potential in control, SARM1-silenced, SARM1-overexpressed, and SARM1(S548A)-expressed N2a cells incubated with or without PrP[106–126]. (E) Western blots of beta 3-tubulin in control, SARM1-silenced, SARM1-overexpressed, and SARM1(S548A)-expressed N2a cells incubated with or without PrP[106–126]. (F) Quantitative results of the data shown in E. Data are expressed as means ± SEM. All assays were repeated three times. **P < 0.01, ***P < 0.001 (one-way analysis of variance followed by Bonferroni's *post hoc* test). ATP: Adenosine triphosphate; GADPH: glyceraldehyde-3-phosphate dehydrogenase; NAD: nicotinamide adenine dinucleotide; ns: not significant; PrP[106–126]: PrP peptide 106–126; SARM1: sterile alpha and Toll-like receptor motif-containing 1; siRNA: small interfering RNA.
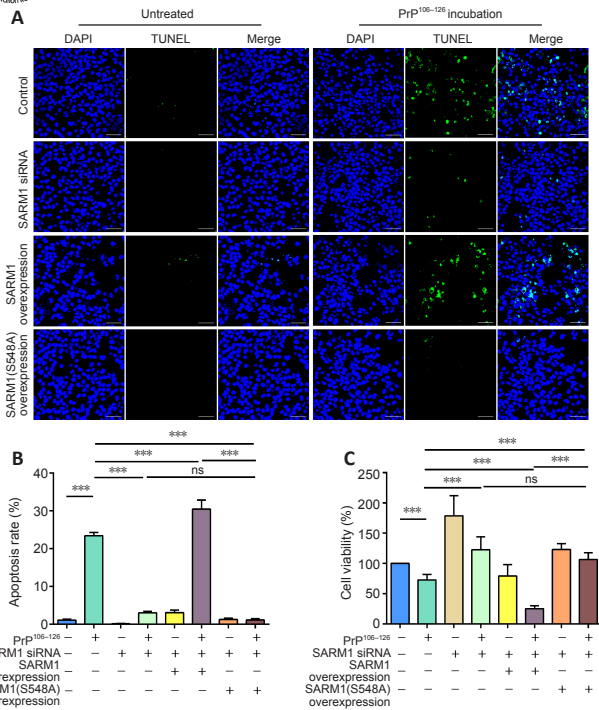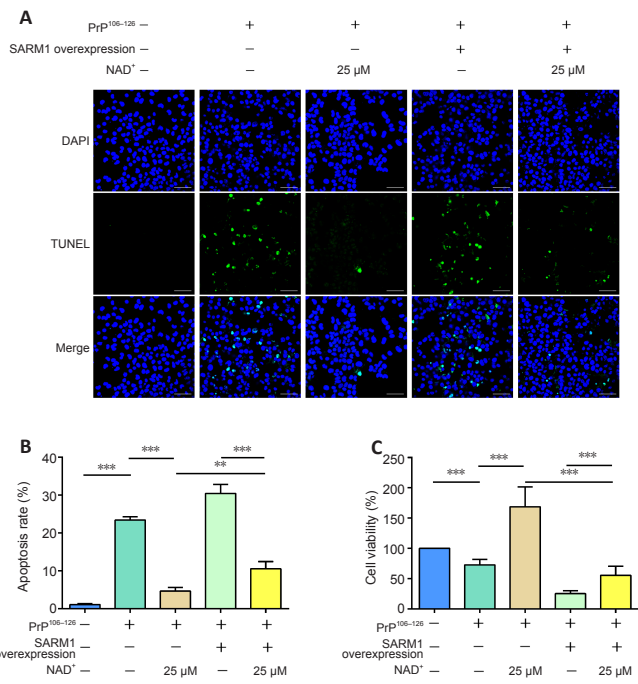
Figure 6 | NADase activity of SARM1 is associated with cell survival following incubation with PrP$^{106–126}$.

(A) TUNEL staining results in control, SARM1-silenced, SARM1-overexpressed, and SARM1(S548A)-expressed N2a cells incubated with or without PrP$^{106–126}$. Incubation with PrP$^{106–126}$ resulted in increased TUNEL stain intensity. SARM1-overexpression enhanced this increase while SARM1-silencing and SARM1(S548A) expression decreased it. Scale bars: 50 μm. (B) Analysis of apoptosis rate for the data shown in A. (C) N2a cell viability was assayed using the cell counting kit-8 kit in control, SARM1-silenced, SARM1-overexpressed, and SARM1(S548A)-expressed cells incubated with or without PrP$^{106–126}$. Data are expressed as means ± SEM. All assays were repeated three times. ***$P < 0.001$ (one-way analysis of variance followed by Bonferroni's *post hoc* test). DAPI: 4′,6-Diamidino-2-phenylindole; NAD: nicotinamide adenine dinucleotide; ns: not significant; PrP$^{106–126}$: PrP peptide 106–126; SARM1: sterile alpha and Toll-like receptor motif-containing 1; siRNA: small interfering RNA; TUNEL: TdT-mediated dUTP nick-end labeling.

Figure 7 | NAD supplementation is protective against the deleterious effects of PrP$^{106–126}$ incubation.

(A) TUNEL staining results of control and SARM1-overexpressed N2a cells incubated with and without PrP$^{106–126}$ and with and without NAD treatment. Incubation with PrP$^{106–126}$ resulted in increased TUNEL stain intensity. In the condition of PrP$^{106–126}$ incubation, NAD+ supplementation decreased the stain intensity; SARM1 overexpression limited the effect of NAD$^+$ supplementation. Scale bars: 50 μm. (B) Analysis of apoptosis rate for the data shown in A. (C) N2a cell viability was assayed using the cell counting kit-8 kit with control and SARM1-overexpressed N2a cells incubated with PrP$^{106–126}$ with or without NAD treatment. Data are expressed as means ± SEM. All assays were repeated three times. **$P < 0.01$, ***$P < 0.001$ (one-way analysis of variance followed by Bonferroni's *post hoc* test). DAPI: 4′,6-Diamidino-2-phenylindole; NAD: nicotinamide adenine dinucleotide; PrP$^{106–126}$: PrP peptide 106–126; SARM1: sterile alpha and Toll-like receptor motif-containing 1; siRNA: small interfering RNA; TUNEL: TdT-mediated dUTP nick-end labelling.

Discussion

Prion disease represents a group of fatal central nervous system diseases that exhibit typical features of neurodegeneration, spongiform vacuolation, and inflammation (Soto and Satani, 2011). The pathogenesis of prion disease remains unclear, but axonal degeneration, mitochondrial dysfunction, and neuronal death have been described and neuronal loss is thought to be the cause of clinical symptoms and death (Hur et al., 2002; Song et al., 2016; Forloni et al., 2019). Evidence from the last decade suggests that SARM1 is associated with axonal degeneration in various pathologic conditions, such as injury, mitochondrial dysfunction, and Leber congenial amaurosis (Osterloh et al., 2012; Gerdts et al., 2013; Summers et al., 2014; Ko et al., 2020; Sasaki et al., 2020). We demonstrated that SARM1 knockdown N2a cells maintained a higher level of axon formation-associated beta-tubulin III expression following PrP$^{106–126}$ incubation. In addition, re-establishing expression of SARM1 led to PrP$^{106–126}$-induced beta-tubulin III loss. SARM1 depletion also protected the axons of primary cultured cortical neurons from the deleterious effects of PrP$^{106–126}$. This finding is in accordance with the studies mentioned above that used other disease models.

Fragmentation of axons and mitochondria after PrP$^{106–126}$ incubation is an indicator of neuronal dysfunction. As the main producer of energy in cells, mitochondria are involved in many neurodegenerative diseases, including Alzheimer's disease, Parkinson's disease, amyotrophic lateral sclerosis, and prion disease (Pacelli et al., 2015; Swerdlow, 2018; Wu et al., 2019; Zhang et al., 2019; Wang et al., 2021). SARM1 function has been associated with mitochondrial respiration and mitochondrial dysfunction-induced cell death (Summers et al., 2014; Murata et al., 2018). As we expected, depletion of SARM1 resulted in maintenance of the axonal and mitochondrial morphology following PrP$^{106–126}$ incubation. Next, we determined whether SARM1 was associated with PrP$^{106–126}$-induced changes in mitochondrial function. We found that downregulation of SARM1 expression limited the effects of PrP$^{106–126}$ on ATP level and MMP. Not surprisingly, overexpression of SARM1 enhanced the PrP$^{106–126}$-induced loss of ATP and reduction of MMP. Overexpression of SARM1 alone does not always lead to axonal damage or mitochondrial dysfunction, which could also be explained by the autoinhibitory nature of the SARM1 protein. Overexpression of SARM1 is just a condition to increase neuronal vulnerability to experimental processing (Gerdts et al., 2013). In an early study, SARM1 was reported to be involved in induction of axonal

degeneration and was associated with intra-axonal mitochondrial dysfunction in the condition of rapid loss of NMNAT2, an enzyme that synthesizes NAD (Loreto et al., 2015). Later studies have explored the NAD$^+$ hydrolase activity of SARM1 from different angles (Gerdts et al., 2015; Essuman et al., 2017; Murata et al., 2018; Horsefield et al., 2019; Bratkowski et al., 2020). Our observation of a marked reduction in the abundance of NAD$^+$ in PrP$^{106–126}$-treated N2a cells suggests that NAD$^+$ metabolism is imbalanced in our *in vitro* model. Many mutation sites with the potential to regulate the NAD$^+$ cleavage activity of SARM1 have been described. The TIR domain of SARM1 is essential for its NADase activity, as mutations E642A and E596K within this domain have been shown to suppress this activity (Essuman et al., 2017; Geisler et al., 2019; Horsefield et al., 2019; Sporny et al., 2020). Ser-548 phosphorylation by JNK is also involved in promoting the NADase activity of SARM1 and switching SARM1 function from promoting mitochondrial transport along axons to inhibiting it (Murata et al., 2018; Xue et al., 2021). We found that PrP$^{106–126}$ failed to induce the loss of NAD$^+$ in SARM1(S548A)-expressed N2a cells; the ATP level and MMP were maintained at relatively high levels in comparison with those of the PrP$^{106–126}$-treated group and SARM1-overexpressed group, and they were not significantly decreased compared with those of the control and SARM1-silenced groups. Therefore, the amino acid substitution at Ser548 suppressed SARM1 NADase activity and limited its further effects on mitochondrial function. These findings illuminate the link between SARM1 activity and mitochondrial dysfunction. Activation of the JNK phosphorylation pathway in prion disease has been previously reported (Carimalo et al., 2005). Further studies of the role of SARM1 in prion disease are warranted. Our finding that NAD$^+$ supplementation rescues PrP$^{106–126}$-induced SARM1-dependent axonal degeneration is in accordance with a previous study that used *in vivo* prion models (Wang et al., 2015). In addition, NAD$^+$ replenishment prevented mitochondrial fragmentation and dysfunction in PrP$^{106–126}$-treated N2a cells.

As shown in previous studies, depletion of SARM1 is protective in different disease models, including injury-induced axonal death (traumatic axonal injury or brain injury), chemotherapy-induced peripheral neuropathy, mitochondrial dysfunction-induced cell death of sensory neurons, and photoreceptor cell death and retinal degeneration in Leber congenial amaurosis type nine (Osterloh et al., 2012; Summers et al., 2014; Geisler et al., 2016; Henninger et al., 2016; Marion et al., 2019; Sasaki et al., 2020) In our study, we found that SARM1 silencing and dysfunctional mutation

rescued PrP$^{106-126}$-induced apoptosis and increased cell survival, while SARM1 overexpression aggravated cell death. However, previous studies have found more muted effects of SARM1 deficiency. In one, SARM1 knockout protected against axonal degeneration only in the early stage of experimental allergic encephalomyelitis, and loss of SARM1 did not promote zebrafish axon resealing nor provide motor neuron protection in an amyotrophic lateral sclerosis animal model (Tian and López-Schier, 2020). Another recent study that used a scrapie mouse model reported that SARM1 deficiency failed to change the prion-induced lesion pattern and did not alter PrP^{Sc} accumulation; instead, SARM1 deficiency upregulated XAF1 and promoted neuronal apoptosis (Zhu et al., 2019). The above findings indicate that the effect of SARM1 deficiency on axons is protective but not restorative and that SARM1 is involved in the early stage of axonal degeneration.

PrP$^{106-126}$ peptide used as a tractable tool of prion disease study may have limitations. Though PrP$^{106-126}$ peptide recapitulated biological features of PrPSc, but was not infectious. There might be unknown differences in the cell response between the peptide and real prion strain. The effectiveness on the basis of studies with PrP$^{106-126}$ can gain disappointing results in clinical trial. It is a very first step to reveal the role of SARM1 NAD$^+$ hydrolase activity in prion disease and the utilization of a new therapeutic strategy. More study *in vivo* with real strains is needed in our future work to confirm our findings.

In summary, our findings demonstrate that prion-induced neuronal damage is partially dependent on the NADase activity of SARM1. We showed that depletion of SARM1, dysfunctional mutation of SARM1, and replenishment of NAD$^+$ protect against axonal degeneration and mitochondrial dysfunction and promote cell survival in an *in vitro* model. Considering that the JNK-c-Jun pathway is activated in prion disease (Carimalo et al., 2005), SARM1 phosphorylation at S548 activates NADase function in injury-induced axonal degeneration (Murata et al., 2018), and SARM1(S548A) is an invalid mutation in PrP$^{106-126}$-induced NAD$^+$ depletion, JNK-SARM1 phosphorylation might be involved in prion disease pathogenesis. The next step is to investigate the mechanisms of SARM1 activation and involvement in prion disease. SARM1 may represent a potential therapeutic target in prion disease.

References

Batlle C, Ventura S (2020) Prion-like domain disease-causing mutations and misregulation of alternative splicing relevance in limb-girdle muscular dystrophy (LGMD) 1G. Neural Regen Res 15:2239-2240.

Bratkowski M, Xie T, Thayer DA, Lad S, Mathur P, Yang YS, Danko G, Burdett TC, Danao J, Cantor A, Kozak JA, Brown SP, Bai X, Sambashivan S (2020) Structural and mechanistic regulation of the pro-degenerative NAD hydrolase SARM1. Cell Rep 32:107999.

Carimalo J, Cronier S, Petit G, Peyrin JM, Boukhtouche F, Arbez N, Lemaigre-Dubreuil Y, Brugg B, Miquel MC (2005) Activation of the JNK-c-Jun pathway during the early phase of neuronal apoptosis induced by PrP106-126 and prion infection. Eur J Neurosci 21:2311-2319.

Collinge J (2001) Prion diseases of humans and animals: their causes and molecular basis. Annu Rev Neurosci 24:519-550.

Essuman K, Summers DW, Sasaki Y, Mao X, DiAntonio A, Milbrandt J (2017) The SARM1 Toll/interleukin-1 receptor domain possesses intrinsic NAD(+) cleavage activity that promotes pathological axonal degeneration. Neuron 93:1334-1343.e5.

Forloni G, Chiesa R, Bugiani O, Salmona M, Tagliavini F (2019) Review: PrP 106-126- 25 years after. Neuropathol Appl Neurobiol 45:430-440.

Galluzzi L, Kepp O, Kroemer G (2012) Mitochondria: master regulators of danger signalling. Nat Rev Mol Cell Biol 13:780-788.

Geisler S, Doan RA, Strickland A, Huang X, Milbrandt J, DiAntonio A (2016) Prevention of vincristine-induced peripheral neuropathy by genetic deletion of SARM1 in mice. Brain 139:3092-3108.

Geisler S, Huang SX, Strickland A, Doan RA, Summers DW, Mao X, Park J, DiAntonio A, Milbrandt J (2019) Gene therapy targeting SARM1 blocks pathological axon degeneration in mice. J Exp Med 216:294-303.

Gerdts J, Summers DW, Sasaki Y, DiAntonio A, Milbrandt J (2013) Sarm1-mediated axon degeneration requires both SAM and TIR interactions. J Neurosci 33:13569-13580.

Gerdts J, Brace EJ, Sasaki Y, DiAntonio A, Milbrandt J (2015) SARM1 activation triggers axon degeneration locally via NAD$^+$ destruction. Science 348:453-457.

Groveman BR, Walters R, Haigh CL (2020) Using our mini-brains: cerebral organoids as an improved cellular model for human prion disease. Neural Regen Res 15:1019-1020.

Gunawardena S, Goldstein LS (2005) Polyglutamine diseases and transport problems: deadly traffic jams on neuronal highways. Arch Neurol 62:46-51.

Henninger N, Bouley J, Sikoglu EM, An J, Moore CM, King JA, Bowser R, Freeman MR, Brown RH, Jr. (2016) Attenuated traumatic axonal injury and improved functional outcome after traumatic brain injury in mice lacking Sarm1. Brain 139:1094-1105.

Horsefield S, Burdett H, Zhang X, Manik MK, Shi Y, Chen J, Qi T, Gilley J, Lai JS, Rank MX, Casey LW, Gu W, Ericsson DJ, Foley G, Hughes RO, Bosanac T, von Itzstein M, Rathjen JP, Nanson JD, Boden M, et al. (2019) NAD(+) cleavage activity by animal and plant TIR domains in cell death pathways. Science 365:793-799.

Hur K, Kim JI, Choi SI, Choi EK, Carp RI, Kim YS (2002) The pathogenic mechanisms of prion diseases. Mech Ageing Dev 123:1637-1647.

Ishikawa T (2021) Saccharomyces cerevisiae in neuroscience: how unicellular organism helps to better understand prion protein? Neural Regen Res 16:489-495.

Ko KW, Milbrandt J, DiAntonio A (2020) SARM1 acts downstream of neuroinflammatory and necroptotic signaling to induce axon degeneration. J Cell Biol 219:e201912047.

Li C, Wang D, Wu W, Yang W, Ali Shah SZ, Zhao Y, Duan Y, Wang L, Zhou X, Zhao D, Yang L (2018) DLP1-dependent mitochondrial fragmentation and redistribution mediate prion-associated mitochondrial dysfunction and neuronal death. Aging Cell 17:e12693.

Li H, Li SH, Yu ZX, Shelbourne P, Li XJ (2001) Huntingtin aggregate-associated axonal degeneration is an early pathological event in Huntington's disease mice. J Neurosci 21:8473-8481.

Loreto A, Di Stefano M, Gering M, Conforti L (2015) Wallerian degeneration is executed by an NMN-SARM1-dependent late Ca(2+) influx but only modestly influenced by mitochondria. Cell Rep 13:2539-2552.

Luo L, O'Leary DD (2005) Axon retraction and degeneration in development and disease. Annu Rev Neurosci 28:127-156.

Marion CM, McDaniel DP, Armstrong RC (2019) Sarm1 deletion reduces axon damage, demyelination, and white matter atrophy after experimental traumatic brain injury. Exp Neurol 321:113040.

Morán M, Moreno-Lastres D, Marín-Buera L, Arenas J, Martín MA, Ugalde C (2012) Mitochondrial respiratory chain dysfunction: implications in neurodegeneration. Free Radic Biol Med 53:595-609.

Murata H, Khine CC, Nishikawa A, Yamamoto KI, Kinoshita R, Sakaguchi M (2018) c-Jun N-terminal kinase (JNK)-mediated phosphorylation of SARM1 regulates NAD(+) cleavage activity to inhibit mitochondrial respiration. J Biol Chem 293:18933-18943.

Osterloh JM, Yang J, Rooney TM, Fox AN, Adalbert R, Powell EH, Sheehan AE, Avery MA, Hackett R, Logan MA, MacDonald JM, Ziegenfuss JS, Milde S, Hou YJ, Nathan C, Ding A, Brown RH, Jr., Conforti L, Coleman M, Tessier-Lavigne M, et al. (2012) dSarm/Sarm1 is required for activation of an injury-induced axon death pathway. Science 337:481-484.

Pacelli C, Giguère N, Bourque MJ, Lévesque M, Slack RS, Trudeau L (2015) Elevated mitochondrial bioenergetics and axonal arborization size are key contributors to the vulnerability of dopamine neurons. Curr Biol 25:2349-2360.

Panneerselvam P, Singh LP, Ho B, Chen J, Ding JL (2012) Targeting of pro-apoptotic TLR adaptor SARM to mitochondria: definition of the critical region and residues in the signal sequence. Biochem J 442:263-271.

Prusiner SB (1991) Molecular biology and transgenetics of prion diseases. Crit Rev Biochem Mol Biol 26:397-438.

Sasaki Y, Kakita H, Kubota S, Sene A, Lee TJ, Ban N, Dong Z, Lin JB, Boye SL, DiAntonio A, Boye SE, Apte RS, Milbrandt J (2020) SARM1 depletion rescues NMNAT1-dependent photoreceptor cell death and retinal degeneration. Elife 9:e62027.

Schneider CA, Rasband WS, Eliceiri KW (2012) NIH Image to ImageJ: 25 years of image analysis. Nat Methods 9:671-675.

Song Z, Zhu T, Zhou X, Barrow P, Yang W, Cui Y, Yang L, Zhao D (2016) REST alleviates neurotoxic prion peptide-induced synaptic abnormalities, neurofibrillary degeneration and neuronal death partially via LRP6-mediated Wnt-β-catenin signaling. Oncotarget 7:12035-12052.

Soto C, Satani N (2011) The intricate mechanisms of neurodegeneration in prion diseases. Trends Mol Med 17:14-24.

Sporny M, Guez-Haddad J, Khazma T, Yaron A, Dessau M, Shkolnisky Y, Mim C, Isupov MN, Zalk R, Hons M, Opatowsky Y (2020) Structural basis for SARM1 inhibition and activation under energetic stress. Elife 9:e62021.

Stokin GB, Goldstein LS (2006) Axonal transport and Alzheimer's disease. Annu Rev Biochem 75:607-627.

Summers DW, DiAntonio A, Milbrandt J (2014) Mitochondrial dysfunction induces Sarm1-dependent cell death in sensory neurons. J Neurosci 34:9338-9350.

Swerdlow RH (2018) Mitochondria and mitochondrial cascades in Alzheimer's disease. J Alzheimers Dis 62:1403-1416.

Tian W, López-Schier H (2020) Blocking Wallerian degeneration by loss of Sarm1 does not promote axon resealing in zebrafish. MicroPubl Biol 2020:2020:2010.17912/micropub.biology.000283.

Wang B, Huang M, Shang D, Yan X, Zhao B, Zhang X (2021) Mitochondrial behavior in axon degeneration and regeneration. Front Aging Neurosci 13:650038.

Wang J, Zhai Q, Chen Y, Lin E, Gu W, McBurney MW, He Z (2005) A local mechanism mediates NAD-dependent protection of axon degeneration. J Cell Biol 170:349-355.

Wang Y, Zhao D, Pan B, Song Z, Shah SZA, Yin X, Zhou X, Yang L (2015) Death receptor 6 and caspase-6 regulate prion peptide-induced axonal degeneration in rat spinal neurons. J Mol Neurosci 56:966-976.

Wu W, Zhao D, Shah SZA, Zhang X, Lai M, Yang D, Wu X, Guan Z, Li J, Zhao H, Li W, Gao H, Zhou X, Qiao J, Yang L (2019) OPA1 overexpression ameliorates mitochondrial cristae remodeling, mitochondrial dysfunction, and neuronal apoptosis in prion diseases. Cell Death Dis 10:710.

Xue T, Sun Q, Zhang Y, Wu X, Shen H, Li X, Wu J, Li H, Wang Z, Chen G (2021) Phosphorylation at S548 as a functional switch of sterile alpha and TIR motif-containing 1 in cerebral ischemia/reperfusion injury in rats. Mol Neurobiol 58:453-469.

Zhang X, Zhao D, Wu W, Ali Shah SZ, Lai M, Yang D, Li J, Guan Z, Li W, Gao H, Zhao H, Zhou X, Yang L (2020) Melatonin regulates mitochondrial dynamics and alleviates neuron damage in prion diseases. Aging (Albany NY) 12:11139-11151.

Zhu C, Li B, Frontzek K, Liu Y, Aguzzi A (2019) SARM1 deficiency up-regulates XAF1, promotes neuronal apoptosis, and accelerates prion disease. J Exp Med 216:743-756.